



This open access document is published as a preprint in the Beilstein Archives with doi: 10.3762/bxiv.2020.32.v1 and is considered to be an early communication for feedback before peer review. Before citing this document, please check if a final, peer-reviewed version has been published in the Beilstein Journal of Nanotechnology.

This document is not formatted, has not undergone copyediting or typesetting, and may contain errors, unsubstantiated scientific claims or preliminary data.

Preprint Title Preparation and Application of Multi-functional His-AA-AuNCs Fluorescent Probe

Authors Shaoguang Li, Jiasong Cai, Yuan Zhang, Peiying Shi, Bing Chen, Liying Huang, Zhen Lin, Xinhua Lin and Hong Yao

Publication Date 25 Mar 2020

Article Type Full Research Paper

Supporting Information File 1 Supporting Information File 1. Optimization of the histidine-chloroauric acid ratio.csv; 31.0 KB

Supporting Information File 2 Supporting Information File 2. Optimization of reaction temperature and time.xlsx; 10.3 KB

Supporting Information File 3 Supporting Information File 3. Determination of different concentrations of H₂O₂.xlsx; 14.7 KB

Supporting Information File 4 Supporting Information File 4. Determination of different concentrations of Fe³⁺.xlsx; 24.4 KB

ORCID® IDs Shaoguang Li - <https://orcid.org/0000-0001-5190-1720>

Preparation and Application of Multi-functional His-AA-AuNCs

Fluorescent Probe

Shaoguang Li^{a, b, c, †}, Jiasong Cai^{a, b, c, †}, Yuan Zhang^{a, b, c}, Peiying Shi^d, Bing Chen^{a, b, c}, Liying

Huang^{a, b, c}, Zhen Lin^{a *}, Xinhua Lin^{a, b, c, *}, Hong Yao^{a, b, c, e *}

^a Department of Pharmaceutical Analysis, School of Pharmacy, Fujian Medical University, Fuzhou, 350122, People's Republic of China;

^b Higher Educational Key Laboratory for Nano Biomedical Technology of Fujian Province, Fujian Medical University, Fuzhou, 350122, People's Republic of China;

^c Nano Medical Technology Research Institute, Fujian Medical University, Fuzhou, 350122, People's Republic of China;

^d Department of Traditional Chinese Medicine Resource and Bee Products, Bee Science College, Fujian Agriculture and Forestry University, Fuzhou, 350002, China;

^e Fujian Key Laboratory of Drug Target Discovery and Structural and Functional Research, Fujian Medical University, Fuzhou, 350122, People's Republic of China.

† Shaoguang Li and Jiasong Cai contributed equally to this work.

* Corresponding authors contact information:

Full addresses: 1 Xue Yuan Road, University Town, Fuzhou Fujian, China. 350122, (Zhen Lin, Xinhua Lin and Hong Yao);

Phone: +86 18060487544

+86 13906909638 (Xinhua Lin);

+86 18259171978 (Hong Yao);

Fax: +86 0591 22862016 (Zhen Lin, Xinhua Lin and Hong Yao);

E-mail: linwenjing002@163.com (Zhen Lin) ;

xhlin1963@sina.com (Xinhua Lin);

yauhung@126.com, or hongyao@mail.fjmu.edu.cn (Hong Yao)

Abstract

Functional nanomaterials with simulated properties have become promising candidates for the detection of hydrogen peroxide. However, there are few studies on the colorimetric detection of metal ions and amino acids based on the peroxidase-simulation activity of amino acid functionalized AuNCs. In this study, a method for preparing fluorescent probe using histidine (His) and ascorbic acid (AA) as reductant and stabilizer was proposed. TMB was used as chromogenic substrate to indicate the catalytic process. The ultraviolet absorbance of oxTMB was determined at the characteristic absorption peak 625nm, and the standard curve was drawn to determine the concentration of H₂O₂ accurately. We found that Fe³⁺ can greatly improve the response signal of His-AA-AuNCs and has high selectivity. The linear range of H₂O₂ concentration detection is 10-9.97×10⁶ μM. The concentration range of probe response to Fe³⁺ is 0.28-280 nM. The His-AA-AuNCs fluorescent probe was applied to intracellular fluorescence imaging after adriamycin injury, and the fluorescence intensity increased with the increase of probe concentration. This study was based on the double-stranded nature of amino acids and the properties of hydrogen peroxide mimic enzymes to detect other substances, which has a promising application prospect, and may potentially be applied to metal ions, amino acids and peptides in the biological and environmental fields in the future.

Keywords: Cell imaging; Colorimetry; Gold nanoclusters; Iron ions; Oxidative mimetic

enzymes.

1. Introduction

Hydrogen peroxide (H_2O_2) is one of reactive oxygen species (ROS). A certain concentration of H_2O_2 can regulate the changes of Ca^{2+} signaling system, cytoplasmic alkalization and K^+ channel, which is an important substance to maintain normal metabolism. However, under the regulation of a variety of external stimuli or intracellular stress, the production of intracellular H_2O_2 increases, and continuous accumulation will lead to a series of oxidative damage behaviors [1]. For example, excessive intracellular H_2O_2 can lead to a variety of inflammatory types, including atherosclerosis [2], chronic obstructive pulmonary disease [3] and hepatitis [4]. Therefore, it is necessary to analyze and detect H_2O_2 with high sensitivity and selectivity. At present, the detection methods of H_2O_2 include laser confocal microscopy [5], ultraviolet spectrophotometer [6], high performance liquid chromatography post-column derivatization [7], chemiluminescence [8] and so on. Laser confocal microscopy has high sensitivity and short time, especially can detect the change of intracellular H_2O_2 concentration, but dynamic monitoring requires low toxicity and strong anti-light drift effect of fluorescent probe, so this method has high requirements for fluorescent probes. Ultraviolet spectrophotometer is a fast and simple method for the determination of intracellular H_2O_2 , the reagent used is inexpensive, the concentration of intracellular H_2O_2 can be determined accurately and quantitatively by making standard curves, but its deficiency is that the sensitivity is not high. Therefore, the colorimetric system is required to have a large response signal and good selectivity in order to improve the detection sensitivity. No matter what kind

of detection method, the signal size and selectivity of the detection probe must be considered.

Therefore, functional nanomaterials with simulated properties have become promising candidates for H₂O₂ detection. Catalytic active nanomaterials (nano-enzymes) show several advantages over natural enzymes, such as simple synthesis, low cost, high regulation, high catalytic activity and good stability under strict conditions [9].

So far [10], developed fluorescent nanomaterials include semiconductor quantum dots, dye-doped nanoparticles, carbon nano-dots and so on. However, compared with these small molecular fluorescent dyes, fluorescent metal nanoclusters, especially fluorescent gold nanoclusters (Au NCs), have the advantages of low toxicity, easy surface modification, strong fluorescence stability and adjustability [11]. Therefore, in the early process of material screening, we mainly used the "bottom-up" preparation method to synthesize gold nanoclusters green and efficiently. We used common ligands 11-MUA [12], cysteine [13], histidine [14] and other compounds as reductants, and added other substances to obtain new gold nanoclusters with better properties and new applications. Finally, histidine-ascorbic acid-gold nanoclusters (His-AA-AuNCs) was successfully synthesized, which has the properties of H₂O₂ mimetic enzymes and could detect H₂O₂ to 10^{-9.97} × 10⁶ μM. The synthesis of the gold cluster was inspired by Chen et al. [15] successfully synthesized the gold cluster with blue-green fluorescence by using histidine as both reducing agent and protective agent for the first time in 2011, and its fluorescence quantum yield was about 8.78%. The synthesis method is simple and rapid. When histidine and chloroauric acid are mixed, electrons are transferred from the imidazole group of histidine to intermediate Au³⁺, then Au³⁺ is reduced to Au atom.

Based on the synthesis of histidine-gold nanoclusters, various compounds were further added, and ascorbic acid was added to increase the fluorescence intensity (Fig. 1A). In 2017, Liu Yan et al. [16] proposed a simple strategy that the peroxidase catalytic activity of His-AuNCs could be inhibited by adding Cu^{2+} , which has a significant linear range of 1-100 nM. Due to the participation of His's imidazole ring, the complex was more stable. A novel and convenient colorimetric nanosensor was established for the detection of Cu^{2+} and histidine. The method is based on the "off-nano" nanoenzyme activity of amino acid functionalized AuNCs, good sensitivity and selectivity were obtained, and the mechanism of "off-detection" system was studied. Previously, there were no reports on the colorimetric detection of metal ions and amino acids based on the peroxidase-mimic activity of amino acid functionalized AuNCs.

It was found that His-AA-AuNCs has a hydrogen peroxide mimic activity. TMB was used as the chromogenic substrate to indicate the catalytic process. The absorbance of oxTMB at 625 nm of the UV characteristic absorption peak was determined. Then the standard curve was made to determine the concentration of H_2O_2 accurately and quantitatively (Fig. 1B).

In the process of application and exploration, we found that His-AA-AuNCs has a wider detection limit of H_2O_2 than the His-AuNCs mentioned above, and Cu^{2+} has no inhibitory effect on its peroxidase catalytic ability, while iron ions can greatly catalyze the mimic enzyme ability to achieve trace detection of Fe^{3+} and be used for cell imaging.

It can be seen from the literature that the research on the colorimetric detection of metal ions and amino acids based on the peroxidase-mimic activity of amino acid functionalized AuNCs is gradually expanding. In the future, this novel "on/off" sensing method, which is

based on the double-chain nature of amino acids and the properties of H₂O₂ mimetic enzymes to detect other substances, might be potentially applicable to metal ions, amino acids and peptides in the field of biology and environment, which has a great prospect.

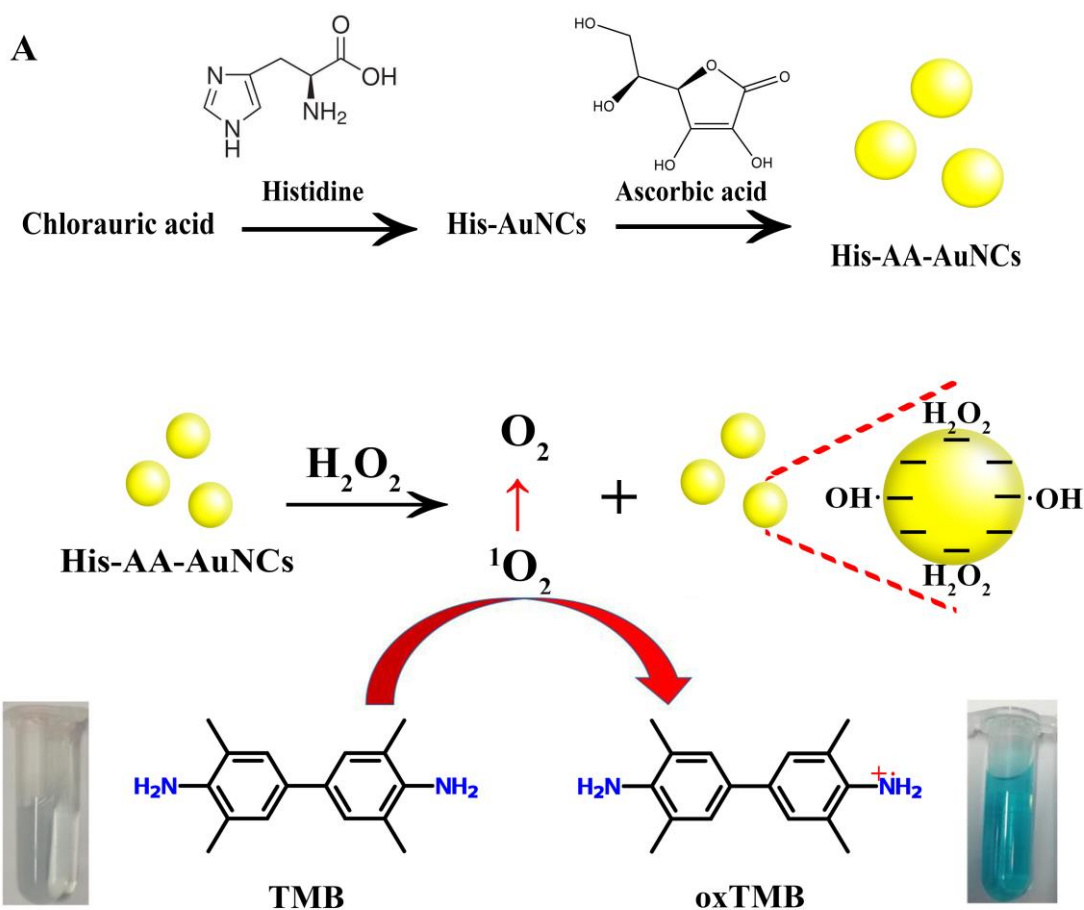


Figure 1: Principles related to experiments. **A**, Synthesis of histidine-ascorbic acid-gold nanoclusters (His-AA-AuNCs). **B**, The reaction principle of His-AA-AuNCs and H₂O₂. Gold clusters reduce hydrogen peroxide to form singlet oxygen, and singlet oxygen causes colorless TMB to oxidize to form blue oxidized TMB.

2. Experimental

2.1 Materials, reagents and instruments

Table 1: Experimental reagent used in this study.

Reagent	Company
L-histidine	Sinopharm Chemical Reagent Co., Ltd. Shanghai, China
Ascorbic acid	Sinopharm Chemical Reagent Co., Ltd. Shanghai, China
3,3',5,5'-tetramethylbenzidine dihydrochloride	Aladdin Biochemical Technology Co., Ltd. Shanghai, China
Chloroauric acid	Aladdin Biochemical Technology Co., Ltd. Shanghai, China
Sodium acetate	Sinopharm Chemical Reagent Co., Ltd. Shanghai, China
Acetic acid	Sinopharm Chemical Reagent Co., Ltd. Shanghai, China

Table 2: Instrument used in this study.

Instrument	Company
UV-2450 UV-Vis Spectrophotometer	Shimadzu, Japan
DKB-501A super constant temperature water tank	Jinghong Experimental Equipment Co., Ltd. Shanghai, China
DF-101S collector type constant temperature Heating magnetic stirrer	Yuhua Instrument Co., Ltd. Gongyi, China

Centrifuge tube	Millipore, the USA
Dmi3000B inverted fluorescence microscope	Leica Microsystem, Germany
FD-1B type freeze dryer	Boyikang Exrimental Instrument Cope., Ltd. Beijing, China
CaryEclipse fluorescence spectrometer	Agilent, the USA
Electronic balance	Sartorius Instrument System Co., Ltd.
PHs-3B precision acidity meter	INESA Scientific Instrument Co., Ltd. Shanghai, China
KQ-218 ultrasonic cleaner	Ultrasonic Instrument Co., Ltd. Kunshan, China
Adjustable pipetting gun	Thermo Fisher Scientific, the USA
Desktop high speed centrifuge	Medical Analytical Instrument Factory, Shanghai, China

Solution preparation

(1) Histidine solution: 1.086 g L-histidine powder was accurately weighed and dissolved in double-steamed water by ultrasound and diluted to 35 mL, and then prepared into 0.2 mol/L.

(2) Ascorbic acid (AA) solution: 0.0176 g ascorbic acid powder was accurately weighed, constant volume to 10 mL with double steamed water, and then prepared into 10 mmol/L.

(3) Chlorauric acid solution: the solid powder of chlorauric acid in the bottle was dissolved in double-steaming water, and then the volume was set to 100 mL. After deducting the empty bottle weight, the total dissolved chlorauric acid powder was 0.9121 g. A 23.16 mmol/L

reserve solution was prepared and stored in a refrigerator for refrigeration and shelter from light. According to the requirement of the experiment, the solution of chloroauric acid with different concentration was diluted with double-distilled water.

(4) Acetate buffer (pH 3.6): 2.04 g sodium acetate powder was accurately weighed, and take 8 mL glacial acetic acid solution, constant volume to 100 mL with double-distilled water, and then adjust it accurately to pH 3.6 with a pH meter.

(5) 3,3', 5,5'-tetramethylbenzidine dihydrochloride solution (TMB): 0.0783 g TMB powder was accurately weighed and prepared into 25 mmol/L with double-distilled water at a constant volume of 10 mL.

2.2 Experimental methods

2.2.1 Preparation and purification of histidine-ascorbic acid-gold nanoclusters

All the glassware used in the experiment were washed and dried thoroughly with freshly Aqua regia.

Chloroauric acid (2 mL, 23.16mM) and ascorbic acid (2 mL, 10 mM) were added sequentially to histidine (5 mL, 0.2M) under stirring. The reaction mixture was incubated at 60°C for 2 hours, then dialyzed with 500Da dialysis bag for 24 hours, and the unreacted small molecules were removed. Finally, the obtained His-AA-AuNCs was stored in a refrigerator at 4°C and kept away from light.

2.2.2 Characterization of His-AA-AuNCs

2.2.2.1 TEM diagram

In this experiment, the morphology and lattice of the samples were observed by field emission high-resolution transmission electron microscope.

2.2.2.2 Infrared spectrum

In this experiment, the surface groups of His-AA-AuNCs were analyzed by Nicolet Avatar 300 Fourier transform infrared spectrometer, and compared with the infrared spectra of histidine and ascorbic acid.

2.2.2.3 XPS spectrum

The X-ray photoelectron spectroscopy (XPS) was used to determine the composition, experimental formula, chemical and electronic states of the elements in the material. In this technique, X-ray is used to irradiate the material to be analyzed, and the kinetic energy and number of electrons escaping from 1nm to 10nm below the material surface are measured at the same time, thus X-ray photoelectron spectroscopy is obtained.

2.2.2.4 Zeta potential analysis

The surface charge of His-AA-AuNCs was measured by laser particle size analyzer (ZetasizerNano) made by Malvern Company, UK.

2.2.3 Application of His-AA-AuNCs intracellular imaging

2.2.3.1 Resuscitation of HepG2 cells

The specific location of the cell cryopreservation tube in the liquid nitrogen tank was

found in the cryopreservation record book. The cell cryopreservation tube was removed from the liquid nitrogen tank and dissolved in warm water at 37°C. To be completely dissolved, the cell suspension was absorbed by a Pap pipette and added to the 10mL centrifuge tube containing 5mL RPMI-1640 medium. 1000rpm centrifugation for 5 minutes, the supernatant was discarded, 8mL fresh RPMI-1640 medium was added, and the cell suspension was blown. The suspension was added to the 75cm² culture flask and cultured at 37°C in 5% CO₂ incubator.

2.2.3.2 Digestion and passage of cells

When the cell covers 90% of the bottom area of the culture flask, it reaches the logarithmic phase and can be passed on. Discard the culture medium in the culture flask, rinse the cell surface with PBS 2mL twice, add trypsin (5%, 1mL) to the culture flask, gently shake so that the trypsin completely covers the cell surface, then rest in the incubator for 2 minutes, observe the cell separation and shrink into a circle under an inverted microscope. Add 4 mL of RPMI-1640 medium to terminate the digestion, and blow the cells gently with a Pap pipette. Place the cell suspension in a 10mL centrifuge tube, centrifuged with 1000 rpm for 5 minutes. Discard the supernatant, add RPMI-1640 medium and to blow into a cell suspension, and then pack the cell suspension into another culture flask, which replenished and cultured at 37°C and 5% CO₂ incubator.

2.2.3.3 Cell count and plating

The cell suspension which was digested and suspended evenly in 0.1mL was mixed in

0.9mLPBS. The uniform cell suspension was absorbed by 10 μ L transfer gun and injected into the cover slide to count the total number of cells (N) in the 4 large cells. The cell concentration is $10^4 N / 4 \times 10$ (dilution multiple), which is the number of cells per milliliter of cell suspension. Then the cell suspension was diluted according to the cell count results, and the cell suspension was diluted into 5×10^4 cells / mL, and added it to a 12-well plate, 1 mL per well, and cultured at 37°C in a 5% CO₂ incubator.

2.2.3.4 His-AA-AuNCs intracellular imaging

The fixed volume was 1 mL, and a series of diluted volumes (4, 8, 16 times) of His-AA-AuNCs were added to the 12-well plate. After incubation for 6 hours, the phenomenon was observed under fluorescence inverted microscope.

2.2.4 Study on the activity of His-AA-AuNCs oxygenase mimics

In order to study the peroxidase-like activity of the prepared His-AA-AuNCs, the reaction time and pH environment of the system were further optimized according to the references of literatures. Add H₂O₂ (90 μ L, 2 M), TMB solution (36 μ L, 25 mM) and His-AA-AuNCs (150 μ L) to acetate buffer (1.5 mL, 0.2M, PH 3.6) in turn, mix well. The solution was bathed at 40°C for 1 hour, and then changed from colorless to blue. Then the solution was transferred for UV spectral scanning.

2.2.5 Detection of Fe³⁺ by His-AA-AuNCs

Prepare a series of acetate buffer solution (1.5 mL) containing different concentration of

ferrous ions, then add H₂O₂ (90 μL, 2 M), TMB solution (36 μL, 25 mM) and His-AA-AuNCs (150 μL), mix well, and set up a negative control group. The mixture was bathed at 60°C for 15 min. Then the solution was transferred for UV spectral scanning and each group was repeated three times.

3. Results and Discussions

3.1 Preparation of His-AA-AuNCs

In this experiment, His-AA-AuNCs was prepared by using histidine as reducing agent and stabilizer, and then adding strong reducing agent ascorbic acid. It is found that the fluorescence intensity of His-AA-AuNCs is better than that of His-AuNCs under the same reaction conditions and time. The optimal excitation wavelength of His-AA-AuNCs is 388 nm and the emission wavelength is 481 nm. It shows blue-green fluorescence under the irradiation of 365nm ultraviolet lamp (Fig. 2A).

Then, the histidine - chloroauric acid ratio is optimized. Fixed concentration of histidine (0.2 M) and chloroauric acid (23.16 mM) were determined according to the ratio of 51.69:1, 19.98:1, 11.50:1, 6.47:1, 3.45:1 and 1.44:1. Adding ascorbic acid (2 mL, 10 mM), water bath at 60°C for 2 hours, then the solution was transferred for fluorescence intensity measurement (Fig. 2B, Supporting Information File 1.). The concentration and reaction time of ascorbic acid were optimized, too (Fig. 2C and D). According to the optimized results, there is the optimum preparation condition: add chloroauric acid (2 mL, 23.16 mM) and ascorbic acid (2 mL, 10 mM) sequentially to histidine (5 mL, 0.2M) under stirring, then incubation at 60°C for 2 hours.

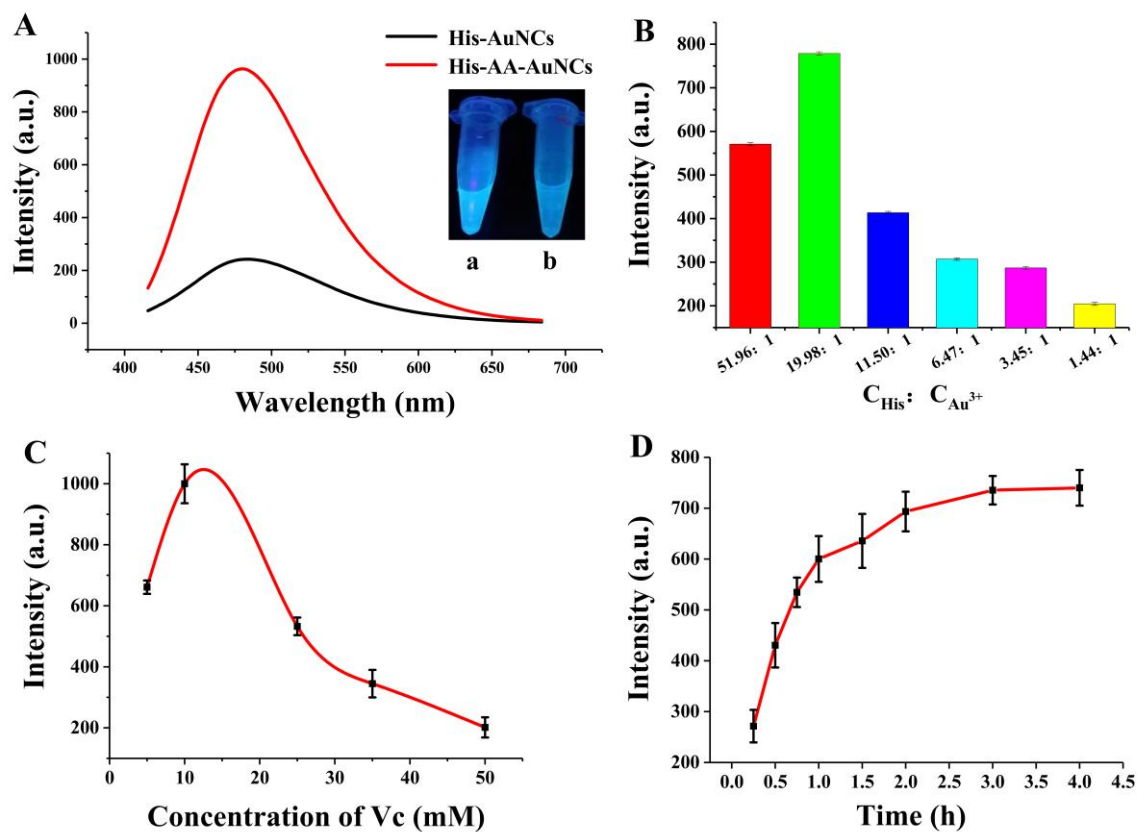


Figure 2: Preparation of His-AA-AuNCs. **A**, Fluorescence emission spectrum of His-AA-AuNCs (red line) and His-AuNC (black line). Inset: photograph displaying the fluorescence of His-AA-AuNCs (a) and His-AuNC (b) upon excitation at 365 nm under a handheld UV lamp. **B**, Histidine-chloroauric acid ratio optimization chart. **C**, Ascorbic acid (AA) concentration optimization chart. **D**, Reaction time optimization chart. The reaction enters the plateau at 2h, which is the optimal optimization time.

3.2 Characterization of His-AA-AuNCs

3.2.1 Morphology standard of His-AA-AuNCs

The morphology and lattice of His-AA-AuNCs were studied by transmission electron microscopy (TEM) (Fig. 3A). His-AA-AuNCs is quasi-spherical in shape and non-uniform in

size, but most of them are 5 nm in diameter. His-AA-AuNCs prepared by this method has obvious lattice fringes, which indicates that the crystallinity of nanoparticles is good.

3.2.2 FT-IR analysis of His-AA-AuNCs

The surface groups of His-AA-AuNCs were analyzed by Nicolet Avatar 300 Fourier transform infrared spectrometer (Fig. 3B). It can be seen that the peak at 2023 cm^{-1} may be $\text{C}\equiv\text{N}$. When the elements of the compound only contain C, H and N, the peak is sharper. When O is closer to $\text{C}\equiv\text{N}$, the peak is weaker, and the peak of His-AA-AuNCs at 2023 cm^{-1} is sharper than that of His, indicating that O is farther away from $\text{C}\equiv\text{N}$ in His-AA-AuNCs. The position of other peaks is basically the same as that of histidine. In the infrared spectrum of histidine, there is a characteristic absorption peak at 1638 cm^{-1} and the peak is sharp, while that of His-AA-AuNCs is the same as ascorbic acid, which may be due to the change of $\text{C}=\text{O}$ to $\text{C}=\text{C}$. In addition, His-AA-AuNCs has a small peak at 3413 cm^{-1} , which is the stretching vibration of O-H, indicating that histidine and ascorbic acid have successfully combined with gold nanoclusters.

3.2.3 Zeta potential analysis of His-AA-AuNCs

The Zeta potential of His-AA-AuNCs solution was detected. Using double distilled water as solvent, the average surface potential was $-0.23 (+0.06\text{ mV})$. When the solvent was PBS buffer, the average surface potential increased negatively with the increase of pH. The results are shown in Table 3, which shows that the His-AA-AuNCs solution is negatively charged.

Table 3: Zeta potential of His-AA-AuNCs under different pH conditions.

pH	Zeta Potential (mV)
3	-3.27 ± 0.46
4	-6.63 ± 1.86
5	-9.2 ± 0.69
6.5	-10.23 ± 1.46
7.4	-12.5 ± 1.39
8.5	-19.63 ± 0.99
10	-17.6 ± 0.53

3.2.4 Living cell imaging of His-AA-AuNCs

After cell resuscitation, the cells were laid in a 12-well plate, then the volume was fixed at 1 mL. A series of diluted His-AA-AuNCs solutions (4, 8, 16 times) were added to the 12-well plate. After incubation for 6 hours, the cells were observed under fluorescence inversion microscopy (Fig. 3C).

Under the excitation of blue light, the green fluorescence of His-AA-AuNCs can be observed clearly in the fluorescence inverted microscope. With the increase of the concentration of gold clusters, the fluorescence intensity increases and the green fluorescence intensity inside and outside the cell is different, indicating that His-AA-AuNCs enters the cytoplasm and even the nucleus.

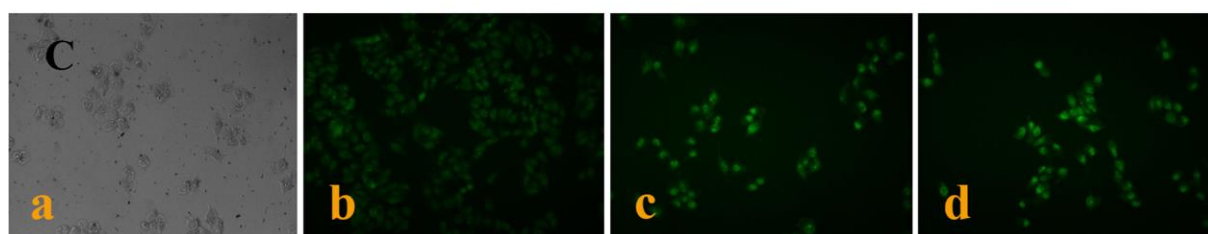
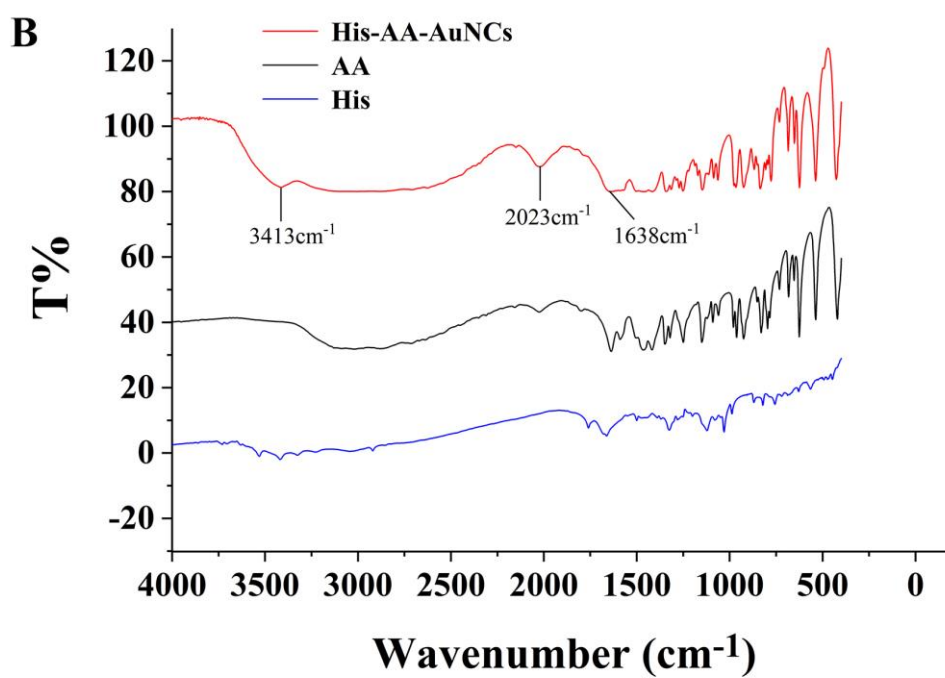
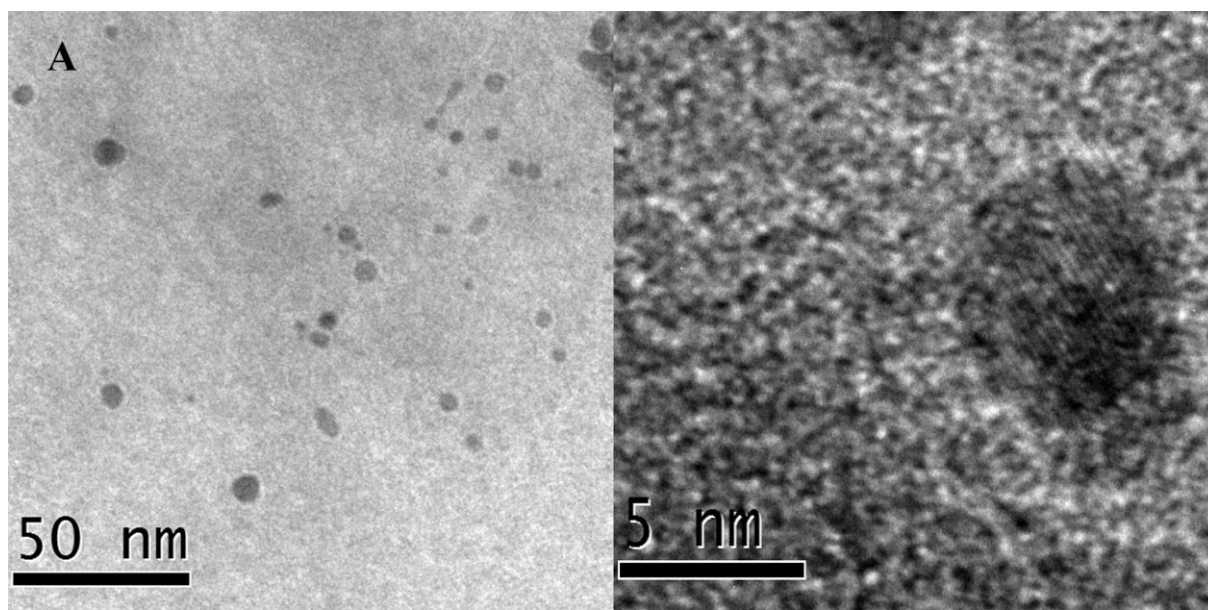


Figure 3: Characterization of His-AA-AuNCs. **A**, Transmission electron micrograph of His-AA-AuNCs. **B**, Infrared spectra of His-AA-AuNCs and single components. **C**, Cell imaging of His-AA-AuNCs in HepG2 (hepatocellular carcinoma) cells. **a**, HepG2 cells in

white field; b, adding 16-fold diluted His-AA-AuNCs; c, adding 8-fold diluted His-AA-AuNCs; d, adding 4-fold diluted His-AA-AuNCs.

3.3 Peroxide mimetic enzyme activity

The content of H₂O₂ produced in cells is closely related to membrane lipid peroxidation, base mutation, DNA strand breakage and protein damage [17-18]. Therefore, it is necessary to detect and analyze H₂O₂ with high sensitivity and selectivity for studying how H₂O₂ participates in various life activities. In this study, we found that His-AA-AuNCs has the mimic activity of peroxidase and can catalyze the oxidation of TMB in the presence of H₂O₂. The concentration of H₂O₂ can be determined by simple colorimetry and ultraviolet spectrophotometer to determine the absorbance of TMB oxidation products at 652 nm.

3.3.1 Determination of H₂O₂

The experimental conditions are optimized. The fixed volume of H₂O₂ (90 μL, 2 M), TMB solution (36 μL, 25 mM) and His-AA-AuNCs (150 μL) were added to the 1.5 mL acetate buffer solution. Four groups of reaction temperatures were set up at 25°C, 40°C, 50°C and 60°C, and the absorbance of each group at 652 nm was measured by ultraviolet spectrophotometer at 5 min, 10 min, 15 min, 30 min, 45 min, 1 h and 1.5 h, respectively (Fig. 4A, Supporting Information File 2.). The increase of temperature can accelerate the system to reach steady-state absorbance, but when the temperature exceeds 50°C and incubates at high temperature for a long time, the steady-state absorbance of the system will decrease, and the original TMB oxidation product will change from blue to green. According to the

experimental results, the optimal experimental condition was selected to incubate 15min at 60°C.

Then, a series of H₂O₂ concentration measurements were carried out, and each group was repeated in three times (Fig. 4B and C, Supporting Information File 3.). the linear range of H₂O₂ was 10-10³ μM, and the regression equation:

$$y = 0.25453 + 1.8728x \quad R^2 = 0.9916 \quad (1)$$

3.3.2 Study on the specificity of hydrogen peroxide mimic enzyme catalyzed by Fe³⁺

It was found that iron ions could catalyze the decomposition of H₂O₂ and significantly increase the peroxide mimetic enzyme activity of His-AA-AuNCs with TMB and H₂O₂ as substrates. In order to further study the selectivity of the detection system, the catalytic activity of other metal ions and other interfering substances was investigated. We measured the absorbance values of Cu²⁺, Ca²⁺, Na⁺, K⁺, Co²⁺, Zn²⁺, adenosine, histidine and dopamine, and compared them with the absorbance value of Fe³⁺ (Fig. 4D). It shows that the increased activity of His-AA-AuNCs-based mimic peroxidase can specifically detect Fe³⁺.

3.3.3 Detection of peroxide simulated enzyme activity of His-AA-AuNCs based on Fe³⁺ positive catalysis

In order to evaluate the sensitivity of the detection system with Fe³⁺ and monitor the change of absorbance. Under the optimum experimental conditions, absorbance values of systems with different concentrations of Fe³⁺ were determined. Taking Fe³⁺ concentration as abscissa, the absorbance ratio (A/A₀) corresponding to Fe³⁺ of each group and blank group at

652 nm as ordinate (Fig. 4E and F, Supporting Information File 4.). The results show that there is a linear relationship between the concentration of Fe^{3+} and A/A_0 in the range of 0.28-280 nM, the regression equation:

$$y = 1.12953 + 0.00378x \quad R^2 = 0.9905 \quad (2)$$

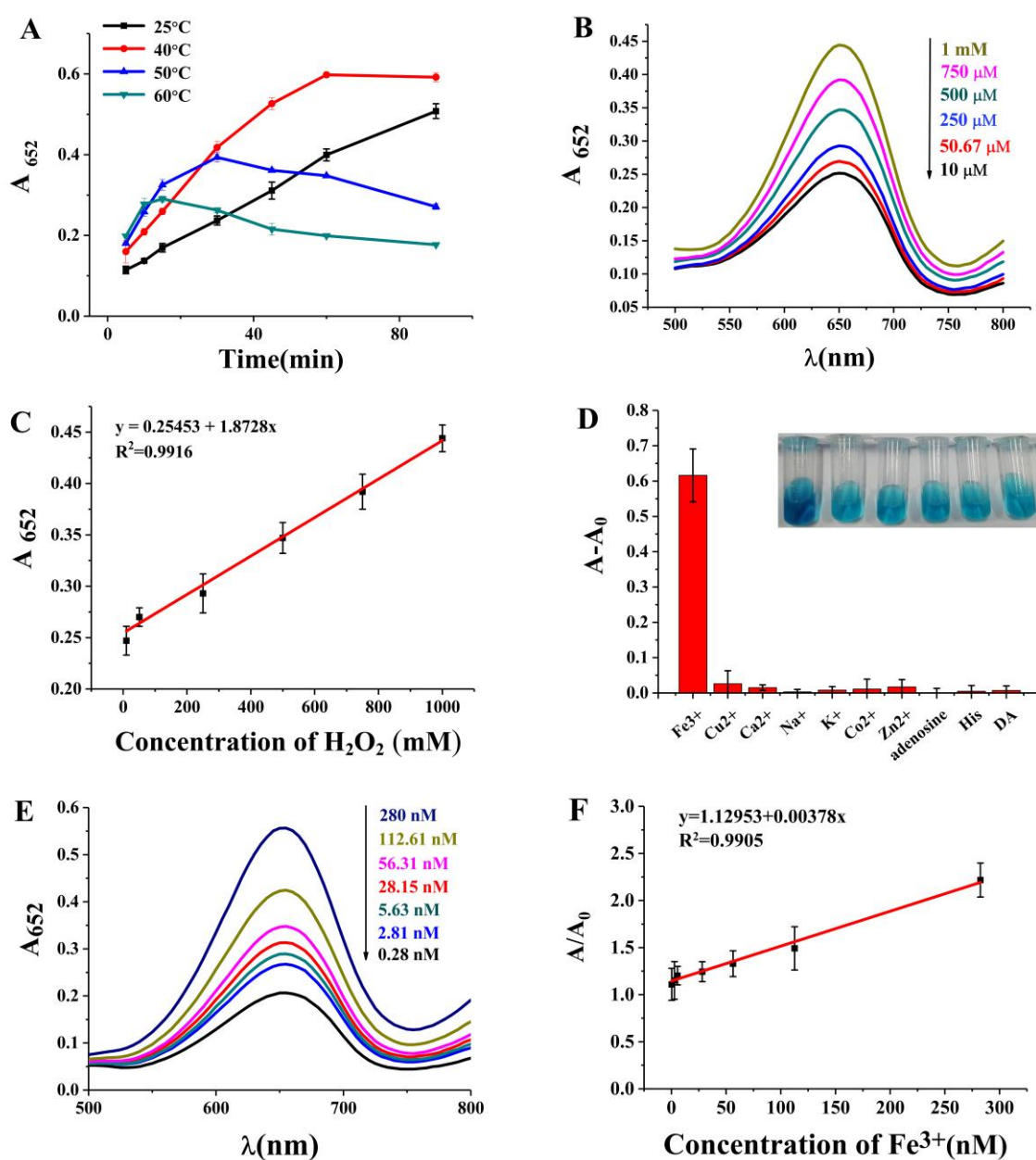


Figure 4: Peroxide mimetic enzyme activity. **A**, Optimization of reaction temperature and time. **B**, Ultraviolet absorbance of His-AA-AuNCs after the addition of H_2O_2 (1 mM-10 μM).

C, Plot of the ultraviolet absorbance of H_2O_2 at 652nm versus the H_2O_2 concentration. **D**, Plot of systems interference experiment. A / A_0 : ultraviolet absorbance of systems with / without metal ion. **E**, Ultraviolet absorbance of His-AA-AuNCs after the addition of Fe^{3+} (280-0.28 nM). **F**, Plot of the ultraviolet absorbance ratio of Fe^{3+} of each group and blank group at 652 nm versus the Fe^{3+} concentration.

3.4 Detection of intracellular reactive oxygen species levels after adriamycin injury

After the cells in the culture flask grew to the logarithmic phase, the cells were laid with 5×10^4 / mL in a 6-well plate, 2 mL per well. After the cells were attached, the adriamycin solution diluted with culture medium (2 mL, final concentrations are 0 μM , 2.5 μM , 5 μM , 10 μM , 20 μM , 40 μM) was added and put into incubator for 6 hours. Then the adriamycin solution was sucked out, and the cells were washed with PBS buffer, then diluted 3 times of His-AA-AuNCs solution was added. After incubation for 5 hours, the phenomena was observed under fluorescence inversion microscope (Fig. 5). Adriamycin can cause autophagy and significantly increase intracellular ROS levels. With the increase of the concentration of adriamycin, the fluorescence intensity under fluorescence inversion microscope becomes brighter, that means the degree of cell injury was deepened, and the level of intracellular ROS increases with the increase of adriamycin concentration.

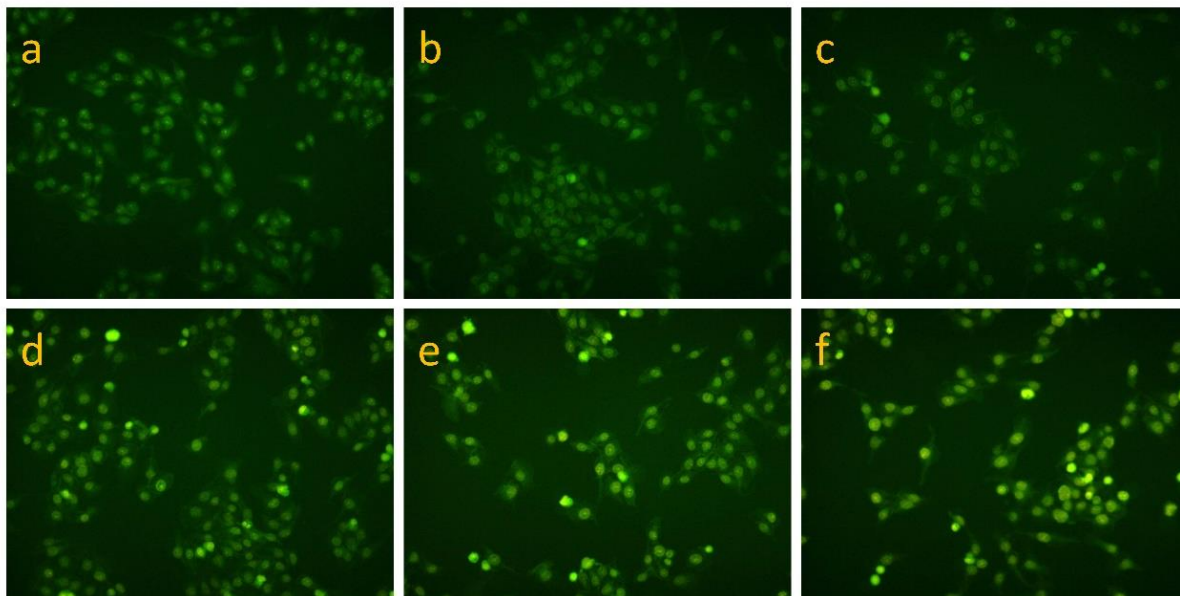


Figure 5: Cell imaging of His-AA-AuNCs in HepG 2 cells injured by adriamycin at different concentrations. a, negative control group; b, 2.5 μM adriamycin intervention; c, 5 μM adriamycin intervention; d, 10 μM adriamycin intervention; e, 20 μM adriamycin intervention; f, 40 μM adriamycin intervention.

4. Conclusions

We designed and synthesized gold nanoclusters His-AA-AuNCs as fluorescent probes by reduction and co-protection of histidine (His) and ascorbic acid (AA). The experiment explored the application field of His-AA-AuNCs and found that the property of hydrogen peroxide mimetic enzyme could be used to detect Fe^{3+} , with high sensitivity and selectivity, and to detect the level of intracellular reactive oxygen species (ROS) after adriamycin injury. The linear range of hydrogen peroxide detection at acellular level was $10\text{-}9.97 \times 10^6 \mu\text{M}$, and the response concentration range to Fe^{3+} was 0.28-280 nM. In the future, the methods for the determination of intracellular H_2O_2 and the function of active fluorescence imaging can be

further developed. His-AA-AuNCs has the advantages of multi-function sample detection, high sensitivity, high selectivity, simplicity and low cost, which broadens the application of gold nanoclusters in the field of life analysis.

Supporting Information

Supporting Information File 1. Optimization of the histidine-chloroauric acid ratio.csv.

Supporting Information File 2. Optimization of reaction temperature and time.xlsx

Supporting Information File 3. Determination of different concentrations of H₂O₂.xlsx

Supporting Information File 4. Determination of different concentrations of Fe³⁺.xlsx

Conflict of Interest

The authors declare no competing financial interest.

Acknowledgments

The authors gratefully acknowledge the financial supports of the National Nature Science Foundation of China (grant numbers 21775023, 81303298 and 81973558), the Joint Funds for the Innovation of Science and Technology, Fujian Province (grant numbers 2017Y9118, 2017Y9123 and 2017Y9124), and the Fujian Provincial Natural Science Foundation (grant numbers 2018J01596).

References

[1] Zhou Liyi; Ding Haiyuan; Zhao Wen; Hu Shunqin. *Spectroc. Acta Pt. A-Molec. Biomolec.*

- Spectr.* **2018**, *206*, 529-534. doi: 10.1016/j.saa.2018.08.042
- [2] Mikhail P. Panchenko; Nilsa Silva; James R. Stone. *Cardiovasc. Pathol.* **2008**, *18*, 167-172. doi: 10.1016/j.carpath.2008.03.008
- [3] Khalil Ansarin; Noe Zamel; Kenneth R. Chapman. *Chest.* **2007**, *132*, No. 4. doi: 10.1378/chest.132.4_MeetingAbstracts.492
- [4] Toro, F.; Conesa, A.; Garcia, A.; Bianco, N. E.; De. Sanctis, J. B. *Clin. Immunol. Immunopathol.* **1998**, *88*, 169-175. doi: 10.1006/clin.1998.4564
- [5] Zhang, X.L.; Wang, P.C.; Song, C.P. *Chin Bull Bot.* **2009**, *44*, 103-106. doi: 10.3969/j.issn.1674-3466.2009.01.012
- [6] Mitsuru Hoshino; Shinichiro Kamino; Mitsunobu Doi; Shingo Takada; Shota Mitani; Rika Yanagihara; Mamiko Asano; Takako Yamaguchi; Yoshikazu Fujita. *Spectroc. Acta Pt. A-Molec. Biomolec. Spectr.* **2014**, *117*, 814-816. doi: 10.1016/j.saa.2013.08.048
- [7] Qi Bin; Tang Xiaoyan; Zhang Yuanhang; et al. *Chin. J. Anal. Chem*, **1998**, *26*, 1041-1046. doi: CNKI:SUN:FXHX.0.1998-09-000
- [8] Xiaohua Li; Zhujun Zhang; Liang Tao; Miao Gao. *Spectroc. Acta Pt. A-Molec. Biomolec. Spectr.* **2013**, *107*, 311-316. doi: 10.1016/j.saa.2013.01.062
- [9] He, W.; Wamer, W.; Xia, Q.; Yin, J.; Fu, P. P. *Environ. Sci. Health, Part C: Environ. Health Sci.* **2014**, *32*, 186-211. doi: 10.1080/10590501.2014.907462
- [10] Wang, F.; Tan, W. B.; Zhang, Y.; et al. *Nanotechnology.* **2006**, *17*, No. 1. doi: 10.1088/0957-4484/17/1/R01
- [11] Yingying Wang; Lihui Hu; Lingling Li; Jun-Jie Zhu. *Journal of Analysis and Testing.* **2017**, *1*, No. 13. doi: 10.1007/s41664-017-0015-7

- [12] Sun, J.; Yang, X. *Biosens. Bioelectron.* **2015**, *74*, 177-182. doi: 10.1016/j.bios.2015.06.013
- [13] Abarghoei Shima; Fakhri Neda; Borghei Yasaman Sadat; Hosseini Morteza; Ganjali Mohammad Reza. *Spectroc. Acta Pt. A-Molec. Biomolec. Spectr.* **2018**, *210*, 251-259. doi: 10.1016/j.saa.2018.11.026
- [14] Zhou You; Tan Hong-peng; Tang Shuang; Hu Zhen-ping; Liang Jian-gong; Ren Guo-lan. *Spectrosc. Spectr. Anal.* **2018**, *38*, 3177-3181. doi: 10.3964/j.issn.1000-0593(2018)10-3177-05
- [15] Yang, X.; Shi, M.; Zhou, R.; et al. *Nanoscale.* **2011**, *3*, 2596-2601. doi: 10.1039/C1NR10287G
- [16] Liu, Y.; Ding, D.; Zhen, Y.; et al. *Biosens. Bioelectron.* **2017**, *92*, 140-146. doi: 10.1016/j.bios.2017.01.036
- [17] Hua, Cai; Kathy, K. Griendling; David, G. Harrison. *Trends Pharmacol. Sci.* **2003**, *24*, 471-478. doi: 10.1016/S0165-6147(03)00233-5
- [18] Asada, K.; Takahashi, M. *Photoinhib. Photosynth.* **1987**, 227-287.